Transportation Research Part D 85 (2020) 102337

Contents lists available at ScienceDirect

Transportation Research Part D

journal homepage: www.elsevier.com/locate/trd

Benefit of speed reduction for ships in different weather conditions

Bhushan Taskar*, Poul Andersen

Technical University of Denmark, Kgs. Lyngby, Denmark

ARTICLE INFO

Keywords:
International Shipping
Greenhouse gas emissions
Speed reduction
Ship performance
Ship emissions
Shipping transport model
Weather routing

ABSTRACT

Currently, the shipping industry is facing a great challenge of reducing emissions. Reducing ship speeds will reduce the emissions in the immediate future with no additional infrastructure. However, a detailed investigation is required to verify the claim that a 10% speed reduction would lead to 19% fuel savings (Faber et al., 2012).

This paper investigates fuel savings due to speed reduction using detailed modeling of ship performance. Three container ships, two bulk carriers, and one tanker, representative of the shipping fleet, have been designed. Voyages have been simulated by modeling calm water resistance, wave resistance, propulsion efficiency, and engine limits. Six ships have been simulated in various weather conditions at different speeds. Potential fuel savings have been estimated for a range of speed reductions in realistic weather.

It is concluded that the common assumption of cubic speed-power relation can cause a significant error in the estimation of bunker consumption. Simulations in different seasons have revealed that fuel savings due to speed reduction are highly weather dependent. Therefore, a simple way to include the effect of weather in shipping transport models has been proposed.

Speed reduction can lead to an increase in the number of ships to fulfill the transport demand. Therefore, the emission reduction potential of speed reduction strategy, after accounting for the additional ships, has been studied. Surprisingly, when the speed is reduced by 30%, fuel savings vary from 2% to 45% depending on ship type, size and weather conditions. Fuel savings further reduce when the auxiliary engines are considered.

1. Introduction

Speed reduction is one of the solutions being proposed at IMO to reduce emissions in the immediate future. Reducing speed is frequently suggested as an important means to reduce the emissions from international commercial shipping (Lindstad et al., 2011; Lindstad and Eskeland, 2015; Woo and Moon, 2014; Norlund and Gribkovskaia, 2013; Lindstad et al., 2013; Fagerholt et al., 2010; Corbett et al., 2009). It is easy to implement as no additional infrastructure is required. The confidence in the measure comes from the observation between 2008 and 2012. During the period, shipping's emissions fell as ships reduced speeds in response to the global economic downturn. A practice that is known as 'slow steaming.'

It is often mentioned that when a ship reduces its speed by 10%, the energy required for the voyage is reduced by 19% (Faber et al., 2012). This approximation is based on the assumption that power (and therefore daily bunker consumption) is proportional to ship speed cubed. Cubic relationship between speed and daily bunker consumption is commonly assumed in maritime transportation models. Psaraftis and Kontovas (2013) have surveyed speed models used in maritime transportation. 25 out of 40 models reviewed, use cubic fuel consumption function. These models are used for weather routing, scheduling, cost optimization, fuel management,

* Corresponding author.
E-mail address: bhta@mek.dtu.dk (B. Taskar).

https://doi.org/10.1016/j.trd.2020.102337

Available online 15 June 2020

and fleet deployment. However, power is proportional to the speed, V, raised to the power of N, where N can range from about 3–6 (Kristensen, 2012). In special cases, the exponent of speed can be as much as 7 (Kristensen, 2018). The speed exponent depends on the hull form and ship speed.

Therefore, a detailed study is required to estimate realistic fuel savings and emission reduction due to reducing the speed. A detailed investigation is necessary to see if the benefits of speed reduction differ with respect to ship type or ship size. Moreover, the effect of different weather conditions should also be considered to make sure that the gains are consistent not just in an ideal calm water condition but also in realistic sea conditions.

Additionally, speed reduction will require an increased number of ships for the same yearly transport work. Increased emissions and fuel consumption due to these extra ships should be taken into consideration while investigating the emission reduction potential. Contrary to the global economic downturn during 2007–2012, seaborne trade is predicted to grow at 3.8% annually between 2018 and 2023 (UNCTAD, 2018). Therefore, compensation for reduced speed using extra ships will play an important role, unlike during 2007–2012.

2. Objective of the paper

The objective is to study the relationship between ship speed and fuel consumption. Results will be compared with the assumption that engine power is proportional to the cube of ship speed. The uncertainty in the estimation of fuel consumption at different ship speeds due to this simple assumption will be quantified. We also aim to investigate if the speed-power relationship varies for different ship types and ship sizes.

It is necessary to investigate if the benefits of speed reduction hold not just in calm water but in realistic weather conditions i.e. in the presence of waves. Therefore, the effect of speed reduction in different weather conditions has been studied.

The speed reduction will likely lead to an increase in the number of ships to compensate for the speed loss and maintain the transport work. The aim is to assess whether mandatory speed reduction will reduce shipping emissions even after increasing the number of ships to keep transport work constant.

3. Case vessels

3.1. Choice of ship types

Container ships, bulk carriers, and tankers together account for 55% of total CO_2 emissions from shipping (Olmer et al., 2017). The contribution of container ships is maximum at 23% followed by bulk carriers (19%) and oil tankers (13%). Therefore, these three ship types were chosen for the investigation.

The container fleet predominantly consists of Feeder, Panamax and Post-Panamax ships in terms of the total number of TEU (MAN Diesel & Turbo, 2013a). As per the Lloyds-Fairplay world ship database for 2007, the category of Post-Panamax container ships is by far the largest CO_2 emitter among different ship categories (Psaraftis and Kontovas, 2009). Therefore, three container ships have been considered, 1100 TEU Feeder, 4000 TEU Panamax, and 8000 TEU Post-Panamax.

In the case of bulk carriers, the maximum deadweight is carried by Capesize vessels followed by Panamax (MAN Diesel & Turbo, 2014). These categories are also responsible for high total CO_2 emissions as compared to other bulk carriers (Psaraftis and Kontovas, 2009). Therefore, a 75,000 dwt Panamax bulk carrier and a 175,000 dwt Capesize bulk carrier have been selected for the analysis. In the case of tankers, VLCCs dominate by far in terms of percentage of total deadweight carried by tankers (MAN Diesel & Turbo, 2013b). VLCC/ULCC cause the largest CO_2 emissions among tanker categories (Psaraftis and Kontovas, 2009). So, one tanker with 300,000 dwt has been chosen. Post-Panamax container ships, Capesize bulk carriers, and VLCC tankers carry out the largest transport work (tonne-km) in the respective ship category.

3.2. Choosing the main dimensions and principal particulars

Ships considered in this paper are representative of the existing shipping fleet. Hull dimensions (length, breadth, and draft), block coefficient (C_B) and the design speeds were calculated using the statistical data of existing container ships (Kristensen and Bingham, 2015a; MAN Diesel & Turbo, 2013a), bulk carriers (Kristensen and Bingham, 2015b; MAN Diesel & Turbo, 2014) and tankers (Kristensen and Bingham, 2015c; MAN Diesel & Turbo, 2013b) of different sizes. Regression formulae for hull dimensions are based on the analysis of the Clarkson database. For estimating the design speeds of container ships, statistics of recent ships (2010–2016) was used since the service speed of container ships decreased after the economic crisis. Principal dimensions of all six ships can be seen in Table 1 and Table 2.

The wetted surface area has been estimated using the formulae given by Kristensen and Bingham (2017). The formulae are based on Mumford's formula (Molland et al., 2011), updated considering 125 newer ships. The updated method has an uncertainty of less than 2% for 89% of the bulk carriers and tankers. Whereas for container ships, the uncertainty is less than 2%, for more than 87% of the ships.

The position of the longitudinal center of buoyancy (LCB), which is essential for resistance calculation, was estimated using the BSRA formula (BSRA, 1971) presented by Molland et al. (2011). The formula calculates LCB location based on the block coefficient. For bulk carriers and tanker, LCB location was also computed using the formula given by Schneekluth and Bertram (1998), which is based on the prismatic coefficient. LCB positions obtained using both the formulae are very similar.

Table 1
Main dimensions of container ships.

		Feeder	Panamax	Post-Panamax
Ship name		C1	C4	C8
TEU	units	1100	4000	8000
L_{pp}	m	142	245	300
B	m	23.5	32.2	43.4
T_{design}	m	8	11.5	13
C_B	–	0.66	0.63	0.635
C_M	–	0.94	0.93	0.93
Design speed	knots	18.1	21.3	23.2
Froude No.	–	0.25	0.22	0.22
Wetted surface	m^2	4357	10325	15673
Thrust deduction	–	0.22	0.17	0.18
Wake fraction	–	0.32	0.28	0.31
Propeller diameter	m	5.15	7.64	8.72
Number of blades	–	4	4	4
Pitch/Diameter	–	0.96	1.00	1.10
Expanded area ratio	–	0.58	0.53	0.65
Design rpm	rpm	122	87	81
Selected engine	–	5S50ME-C8.5	7S70ME-C10.5	7G90ME-C10.5
MCR power	kW	7641	19034	40066
MCR speed	rpm	126	90	83

Table 2
Main dimensions of bulk carriers and tanker.

		Bulk carriers		Tanker
		Panamax	Capesize	VLCC
Ship name		B75	B175	T300
Maximum deadweight[a]	ton	75,000	175,000	300,000
L_{pp}	m	220	280	320
B	m	32.25	45	60
T_{design}	m	12.2	16.5	20.4
C_B	–	0.855	0.85	0.82
C_M	–	0.97	0.98	0.98
Design speed	knots	14.6	15	15.8
Froude No.	–	0.162	0.147	0.145
Wetted surface	m^2	11155	19467	28111
Thrust deduction	–	0.21	0.21	0.21
Wake fraction	–	0.39	0.38	0.34
Propeller diameter	m	6.81	8.39	9.76
Number of blades	–	4	4	4
Pitch/Diameter	–	0.63	0.65	0.68
Expanded area ratio	–	0.53	0.48	0.46
Design rpm	rpm	112	90	80
Selected engine	–	9S50ME-C9.7	7S65ME-C8.6	5S90ME-C10.5
MCR power	kW	11904	18657	28969
MCR speed	rpm	115	93	82

[a] Maximum deadweight is based on scantling draft.

Thrust deduction fraction and wake fraction were estimated using Harvald's method (Harvald, 1983). However, Harvald's method gives higher wake fraction and thrust deduction fraction for bulk carriers and tankers (Kristensen and Bingham, 2017). Therefore, corrections by Kristensen and Bingham (2017) were used. The corrections are based on model tests of 26 bulk carriers and tankers. For 42% of the ships, wake fraction is within 10% accuracy and for 38% of the ships, thrust deduction fraction is within 10% accuracy compared to model tests. Uncertainty in wake fraction and thrust deduction fraction is relatively large as these parameters are highly

dependent on the shape of hull especially near the stern. Thrust deduction fraction and wake fraction have been assumed constant in the current work. Uncertainty due to this assumption has been studied by Taskar et al. (2019a). The midship section coefficient was estimated using an approximation suggested by Molland et al. (2011). All ships were assumed to have a bulbous bow.

3.3. Selecting engine and propeller

Engine and propeller have been designed simultaneously, considering engine-propeller matching. An iterative procedure was required between engine selection and propeller design.

The procedure given by MAN Energy Solutions (2018) has been followed for choosing appropriate engines. The engines for all ships are considered to be two-stroke diesel engines directly coupled with the propeller. The engine power has been calculated at design speed in calm water. MCR power and rpm were obtained by considering 15% sea margin, 10% engine margin and 5% light running margin for all the ships. MCR power was compared with the installed power of similar existing ships (MAN Diesel & Turbo, 2013a; MAN Diesel & Turbo, 2014; MAN Diesel & Turbo, 2013b). In all the cases, calculated MCR power matches the statistically obtained installed power for existing ships of similar deadweight or TEU. A good match between prediction and installed power of existing ships also serves as a validation for all the intermediate variables estimated using a variety of different methods from various sources. The CEAS engine calculation tool provided by MAN Energy Solutions has been used for choosing the engines (MAN Energy Solutions, 2019). Engine details like specific fuel consumption (SFOC) at different loads are also obtained from MAN Energy Solutions (2019). SFOC values are given considering marine diesel as a fuel. Details of selected engines have been provided in Tables 1 and 2.

B-series propellers have been designed for each ship considering the required thrust, propeller diameter and the rpm range of engine layout diagram. The required thrust was obtained using calm water resistance calculations (Section 5.1) and thrust deduction fraction. Propeller diameters have been selected using the statistical data of existing ships (Kristensen and Bingham, 2017). The formulae are based on the regression analysis of significant ships (1990–2010) database. Propeller rpm and pitch ratio have been optimized for maximum efficiency at the design speed in the calm water condition, which is the procedure generally followed for designing the propellers (MAN Energy Solutions, 2018). Principal particulars of the designed propellers can be found in Tables 1 and 2. Open water curves are presented in Fig. 1.

4. Route and weather data

Weather data are required to simulate ships in different weather conditions. The weather data averaged for each month in the year 2010 have been obtained from ECMWF (Copernicus Climate Change Service (C3S), 2017). The data consist of significant waveheight, peak period and wave direction at different latitudes and longitudes. The resolution of the data is 1 degree.

The route from Los Angeles to Osaka has been chosen as the weather conditions vary significantly along this route in different seasons. Therefore, the effect of a variety of different weather conditions on vessel performance can be observed. The route along with average weather conditions in January can be seen in Fig. 2. The plot has been colored as per significant waveheight and wave directions can be seen as blue arrows. The weather along the route was obtained by interpolating the weather data. Significant waveheight and peak period at multiple points along the route in different months can be seen in Fig. 3.

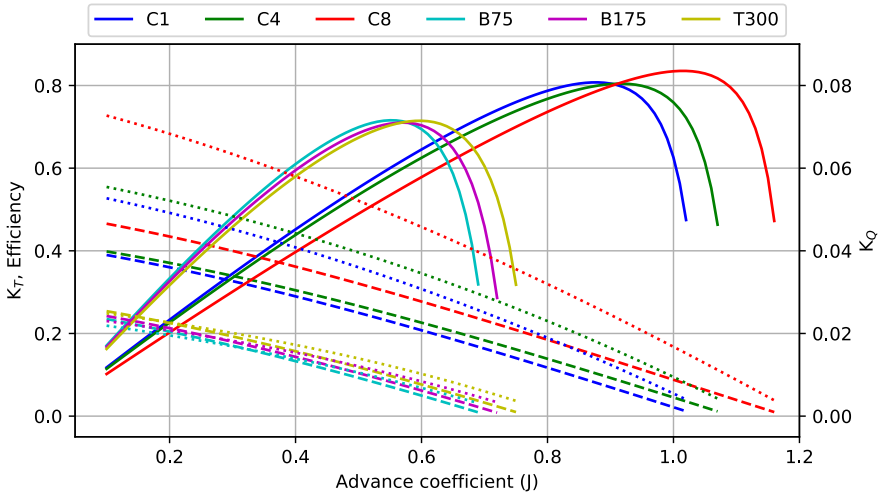

Fig. 1. Open water curves of propellers designed for each ship.

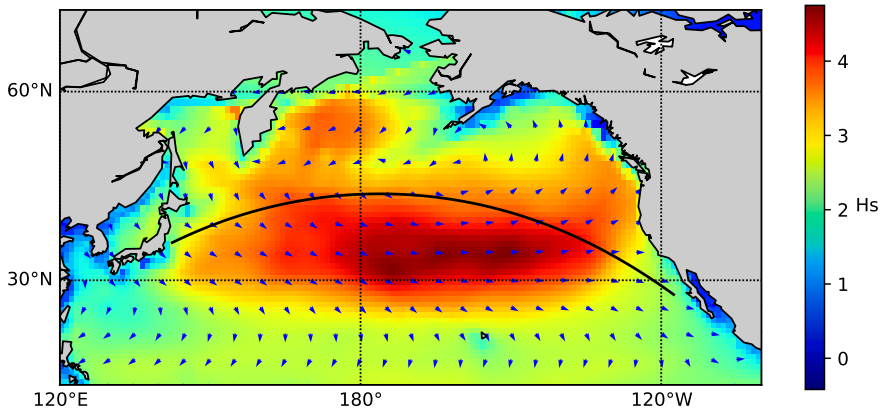

Fig. 2. Average weather in January (Significant waveheight and wave directions) along with the route from Los Angeles to Osaka (Copernicus Climate Change Service (C3S), 2017).

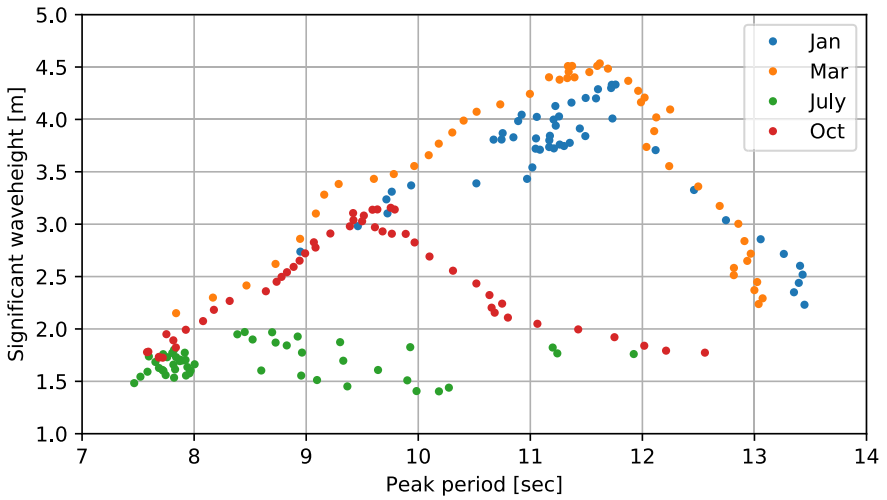

Fig. 3. Significant waveheight and peak period of waves at multiple points along the route in different months (Copernicus Climate Change Service (C3S), 2017).

5. Methods used for vessel performance estimation

5.1. Calm water resistance

Guldhammer and Harvald's method (Harvald, 1983; Guldhammer and Harvald, 1974) updated by Kristensen and Bingham (2017) has been used for the estimation of calm water resistance. The empirical resistance method is based on model test results from multiple model basins to estimate residuary resistance. The residuary resistance coefficient is given as a function of the length-displacement ratio, prismatic coefficient, and Froude number. Corrections are applied based on B/T, LCB position and bulbous bow parameters. The corrections suggested by Kristensen and Bingham (2017) are based on the model tests of newer ships. Friction resistance is calculated using the ITTC 1957 skin friction line as suggested by Guldhammer and Harvald (1974). The residual resistance coefficient and friction resistance coefficient together give the total resistance coefficient (C_T) in calm water.

The method has been validated for four ships using experimental data. Calm water resistance data from model tests are available for KCS and KVLCC2 from the Gothenburg workshop on CFD in ship hydrodynamics (Larsson et al., 2014). Resistance data from model tests for DTC and HTC are taken from el Moctar et al. (2012) and Bertram et al. (1994) respectively. The Duisburg test case (DTC) is a 14000 TEU Post-Panamax container carrier and the Hamburg test case (HTC) is a 150 m container ship. Both are often used as benchmark cases for validation. Full-scale resistance coefficients are obtained using the ITTC (1978) method. Resistance coefficients calculated using the updated Guldhammer and Harvald's method have been compared with the ones obtained from model tests (Fig. 4).

Calculations using the updated Guldhammer and Harvald's method show a good correlation with the experimental results. Variation of calm water resistance at different ship speeds is correctly predicted for various ship types and sizes. Therefore, the method can be used for studying the effect of ship speed on the performance. The HTC container ship is similar to the container ship

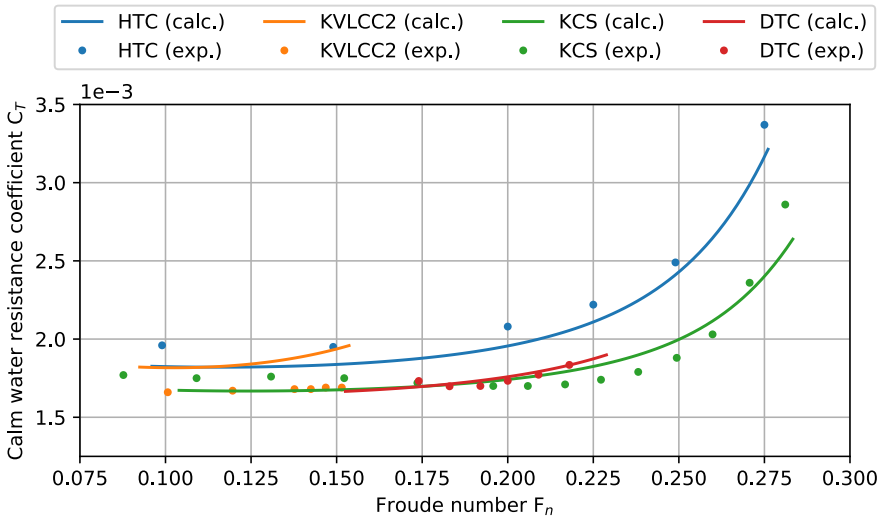

Fig. 4. Validation of the updated Guldhammer and Harvald's method using experimental results.

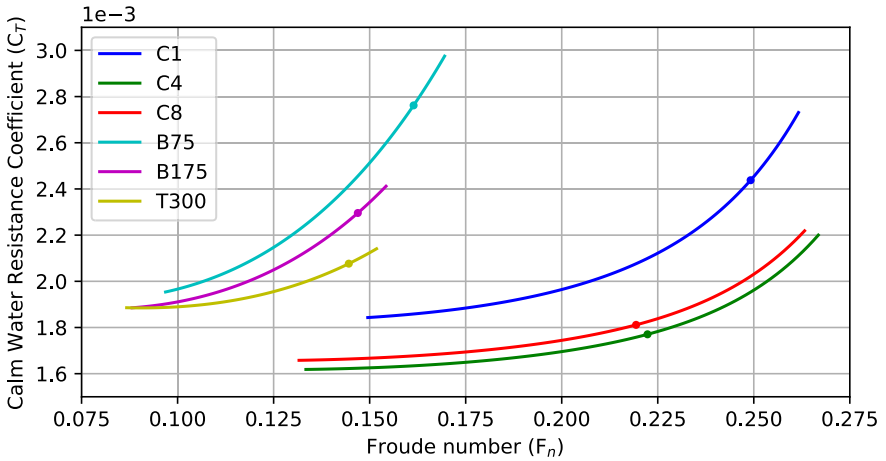

Fig. 5. Calm water resistance coefficient C_T at a range of Froude numbers. (dots: design point).

C1 considered in this study. The KCS is similar to C4 and the size of KVLCC2 is similar to T300.

The calm water resistance coefficient calculated for each ship can be seen in Fig. 5. The container ship C1 shows much higher C_T as compared to the other two container ships C4 and C8. The higher C_T is due to a much lower length-displacement ratio (5.5 as compared to 6.4 and 6.3) and a higher prismatic coefficient (0.7 as compared to 0.68).

Generally, C_T is considered constant which leads to the assumption of daily bunker consumption proportional to V^3, as fuel consumption is proportional to average power. However, it is observed that C_T is constant for speeds much lower than the design speeds. It increases sharply for higher Froude numbers. In all the cases, C_T has significant Froude number dependence around the design speed of the ships. The dependence of C_T on ship speed is crucial for the estimation of fuel consumption or emissions. It is also observed that the C_T curve gets steeper as ship size decreases. As resistance trends depend on types and sizes of ships, speed reduction will be more advantageous for some ships depending on their shape, size, and operating profile.

Guldhammer and Harvald's method can estimate the variation of total resistance coefficient (C_T) at different ship speeds. Therefore, it provides more accurate modeling of power as a function of ship speed compared to constant C_T assumption. As observed by Kristensen (2018), power can be proportional to V^N, where N can vary from 3 to 7. Often N is approximated to 3 which is not accurate. Residual resistance plots provided by Harvald (1983) can be used for the estimation of N using principal particulars of a ship.

5.2. Added resistance in waves

Added resistance in waves is required for the estimation of power in the presence of waves. The method developed at the Technical University of Denmark (DTU) has been used for estimating added resistance (Martinsen, 2016; Nielsen, 2015). The method is based on the interpolation of multiple simulations carried out for different ship geometries. The method uses a combination of strip

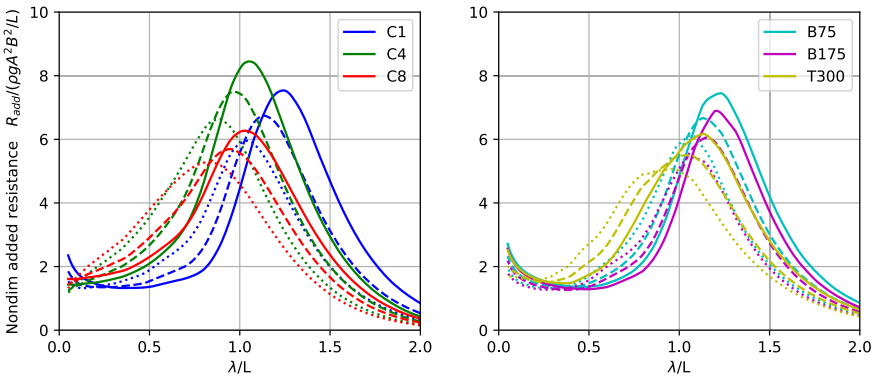

Fig. 6. Added resistance RAOs for all ships at different ship speeds in head waves. (solid line: design speed, dashed line: 80% of design speed, dotted line: 60% of design speed).

theory (Salvesen, 1978), Faltinsen's method (Faltinsen et al., 1980) for short waves and WAMIT calculations (Lee and Newman, 2013) for zero forward speed cases. A detailed description and the validation of the method for multiple ships has been presented by Martinsen (2016) and Nielsen (2015). A comparison of added resistance RAOs calculated using different methods (including DTU method) and experiments has been studied by Taskar et al. (2019b).

The DTU method calculates added resistance in waves based on the main dimensions of the ship, wave condition (waveheight, period and wave direction) and ship speed. Dependence of added resistance on ship speed is critical for the current study. The method can consider wave directions from head seas to beam seas. Added resistance has been neglected in stern quartering and following sea conditions.

Added resistance computations for all six ships can be seen in Fig. 6. Added resistance has been non-dimensionalized by $\rho g A^2 B^2/Lpp$, where A, B, and Lpp are wave amplitude, ship breadth and ship length respectively. The results have been presented for three different ship speeds, all in head sea condition. In all the cases, the peak of added resistance RAO decreases and shifts to a lower wavelength as the speed decreases.

In the route simulations, added resistance has been computed in irregular waves. Significant waveheight and peak period are used to construct a Bretschneider spectrum. Wave spectrum and added resistance RAO are then used to calculate added resistance in irregular waves.

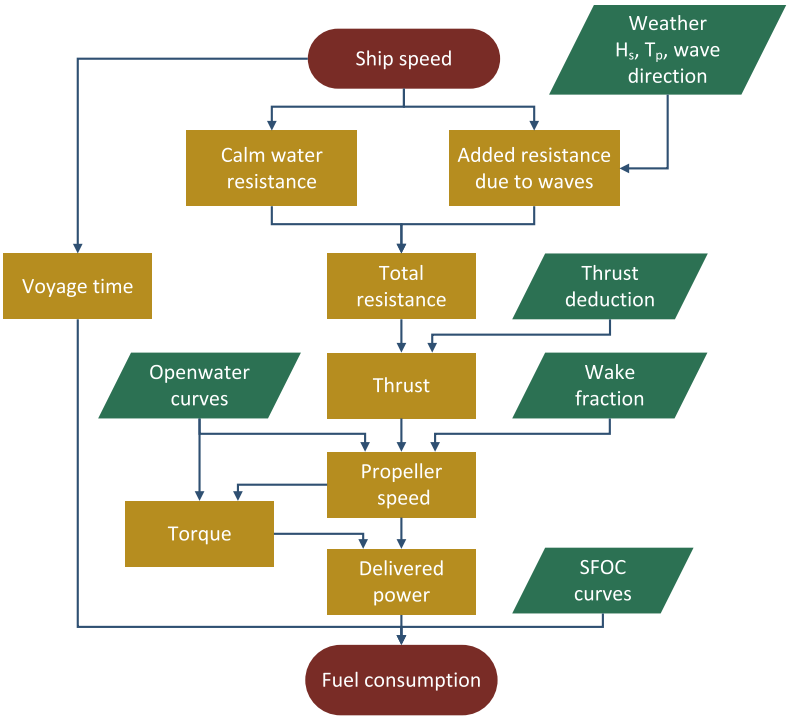

Fig. 7. Voyage simulation methodology.

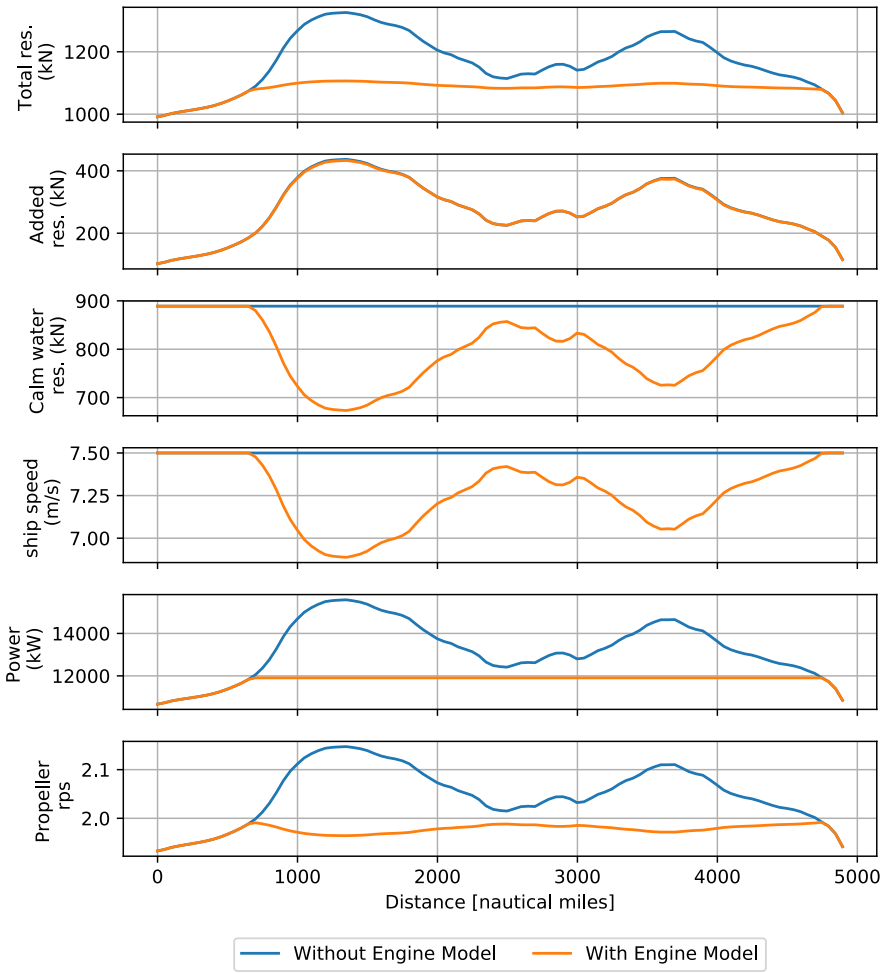

Fig. 8. Performance of B75 ship going from Los Angeles to Osaka in average weather of January. Simulations with and without engine model have been presented.

6. Simulation methodology

Voyages have been simulated to calculate the total fuel consumption of a vessel on a given voyage. An overview of this methodology can be seen in Fig. 7. Calculations have been performed at multiple points along the route, spaced 50 nautical miles apart. Calm water resistance is computed based on the ship speed. Added resistance in waves is calculated using ship speed and wave conditions at the location. Thrust requirement is then estimated based on total resistance and thrust deduction fraction. Thrust, propeller open water curves and wake fraction are used to compute propeller rate of rotation, torque and hence delivered power. Therefore, changes in propeller efficiency at different ship speed and propeller speed are taken into consideration. Finally, fuel consumption for the voyage is obtained using engine power and SFOC curves. An example of simulation result is presented in Fig. 8.

The engine model has been used in the simulations to make sure that engine power and rpm are within the limits of the engine load diagram. Ship speed is reduced if available power is lower than the required power. Engine load diagrams have been obtained from the CEAS engine calculation tool provided by MAN Energy Solutions (2019). The effect of the engine model can be seen in the example calculation presented in Fig. 8. In the case of simulation with the engine model, the ship speed drops when the maximum power of the engine is reached.

7. Simulations, results and discussion

Voyages have been simulated for all six ships at multiple speeds to study the benefits of speed reduction. Initially, simulations were performed considering a calm water condition without the engine model. Dependence of fuel consumption on ship speed has been studied for different ships. The engine model was then included to consider the variation of SFOC at different engine loads and to include actual attainable ship speeds. Finally, multiple voyages were simulated in different weather conditions to find the impact of weather on fuel consumption at different speeds.

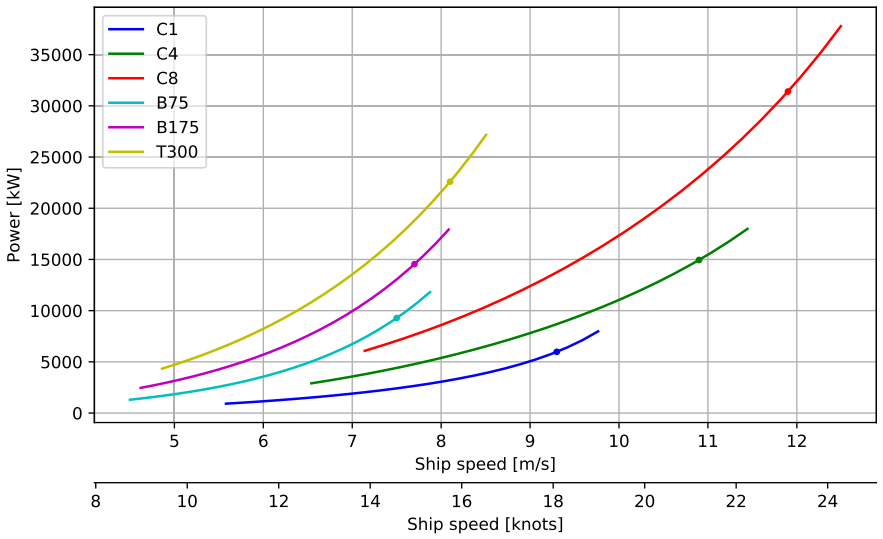

Fig. 9. Speed power curve for all the ships. (dots: design point).

7.1. Fuel consumption in calm water at different ship speeds

Initially, the ships have been assumed to sail in calm water. Speed-power curves in calm water can be seen in Fig. 9. All ships have been simulated for speeds ranging from 70% to 100% of the design speed. The percentage reduction in fuel consumption has been calculated at each speed compared to the fuel consumption at the design speed. The specific fuel consumption of the main engine is assumed constant. Fig. 10 depicts the relationship between speed reduction and the reduction in fuel consumption. Fuel savings due to speed reduction vary for different ships. Percentage speed reduction and fuel savings are calculated as follows:

$$\%\ \text{speed reduction} = \frac{V_1 - V_0}{V_0} \times 100$$

$$\%\ \text{fuel savings} = \frac{FC(V_1) - FC(V_0)}{FC(V_0)} \times 100$$

where, FC is the fuel consumption of a voyage at a certain ship speed. V_0 is the design speed of the ship and V_1 is the speed at which the voyage is simulated.

A cubic relationship is commonly assumed between ship speed and power for shipping transport models (Psaraftis and Kontovas, 2009; Lindstad et al., 2011). In very few cases like Du et al. (2011), the exponent other than 3 is used. Therefore, additional reference curves have been plotted in Fig. 10, assuming $P \propto V^3$, $P \propto V^4$ and $P \propto V^5$. Curves for all the ships deviate significantly from the curve

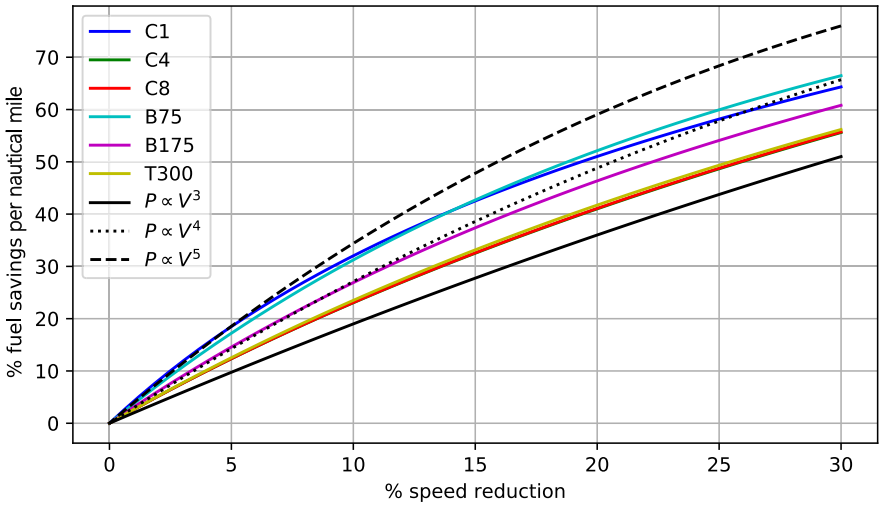

Fig. 10. Relationship between fuel savings and speed reduction for the ships along with fuel savings obtained assuming that the power is proportional to V^3, V^4 and V^5.

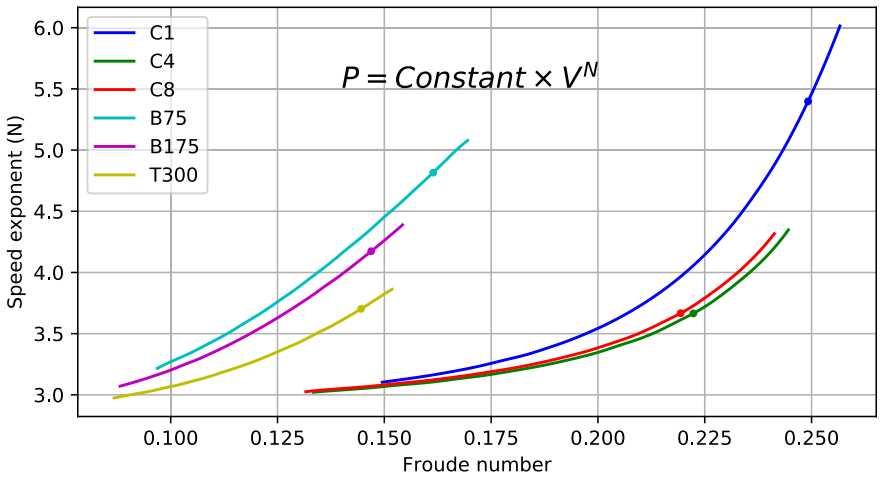

Fig. 11. Speed exponent for different ships as a function of Froude number. (dots: design point).

Table 3
Average speed exponents for ship speeds ranging from $0.7V_o$ to V_o. (V_o: design speed).

Ship name	C1	C4	C8	B75	B175	T300
Speed exponent (N)	4.0	3.3	3.3	4.2	3.7	3.4

assuming power proportional to ship speed cube. The largest deviation can be observed in the case of B75 (75,000 dwt bulk carrier) and C1 (1100TEU container ship). At 10% speed reduction, they show more than 30% fuel savings instead of 19% predicted by $P \propto V^3$ assumption. In some cases, the power seems proportional to V^4 or even V^5 depending on ship type and operating speed. The cubic assumption would provide a conservative estimate of fuel savings in calm water.

Assuming, the power is proportional to V^N, where N is speed exponent, N itself seems dependent on ship speed. To investigate the speed dependence, the speed exponent has been computed at multiple Froude numbers for each ship as seen in Fig. 11. The speed exponent at speed $V_{i+\frac{1}{2}}$ is calculated using two closely spaced points (V_i, P_i) and (V_{i+1}, P_{i+1}), where the subscript i denotes i^{th} point on the speed-power curve. The speed exponent at $V_{i+\frac{1}{2}}$ is calculated as follows:

$$N_{i+\frac{1}{2}} = \frac{log\left(\frac{P_i}{P_{i+1}}\right)}{log\left(\frac{V_i}{V_{i+1}}\right)}$$

The observations in Fig. 10 can be explained using Fig. 11. The assumption of the cubic relationship between power and ship speed does not work for all ships at all speeds. Importantly, the speed exponent can deviate from 3 even well within the operating speed ranges. Such an assumption can cause significant discrepancies in the computation of fuel consumption especially when the voyage speed is to be optimized.

Speed exponents have also been computed for speed-power curves in Fig. 9 using curve fitting. Power is considered proportional to V^N, where V is a ship speed. Speed exponents can be seen in Table 3. It is observed that the fit underestimates the power at the lower and higher end of the curve in each case. The average speed exponent obtained by fitting the entire speed-power curve is much closer to 3 (Table 3) as compared to speed exponents obtained at each point as in Fig. 11. Wang and Meng (2012) also obtained speed exponents varying from 2.7 to 3.3 using the full-scale data. This is likely because an average of speed exponent was calculated by curve fitting instead of calculating speed exponent at different ship speeds.

The cubic relationship is often used to simplify computations in optimization algorithms. However, one must be aware of possible errors (up to 15%) in estimating fuel consumption. Estimation of bunker consumption could be improved using Guldhammer and Harvald's method (Guldhammer and Harvald, 1974; Kristensen and Bingham, 2017) which can capture important trends in resistance based on principal particulars (displacement, prismatic coefficient (C_P)) and ship speed.

7.2. Influence of engine efficiency at different loads

In the previous section, engine efficiency or specific fuel consumption(SFOC) was assumed constant. However, SFOC depends on engine load. Engines running at a low load, due to speed reduction, will have higher SFOC. Therefore, the effect of load-dependent SFOC should be included while calculating fuel savings due to speed reduction.

Engine fuel consumption at different loads can be seen in Fig. 12. In the current study, all the engines are tuned for a high load;

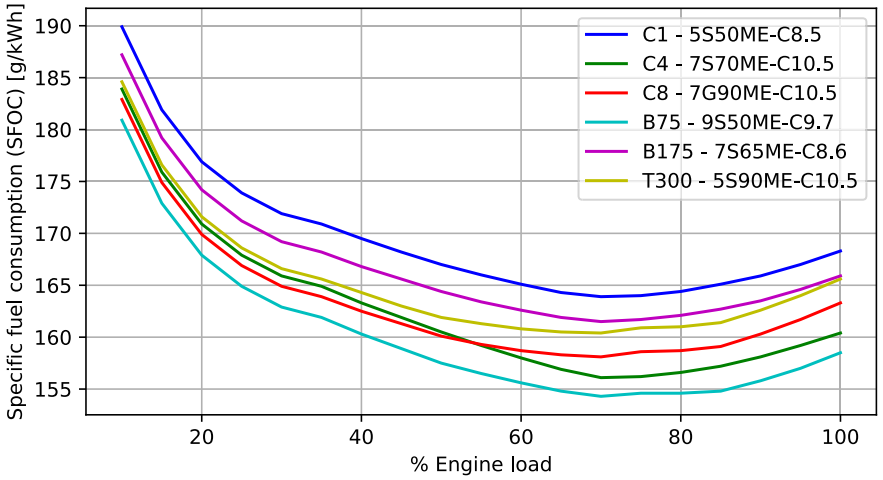

Fig. 12. Specific fuel consumption of the engines at different loads.

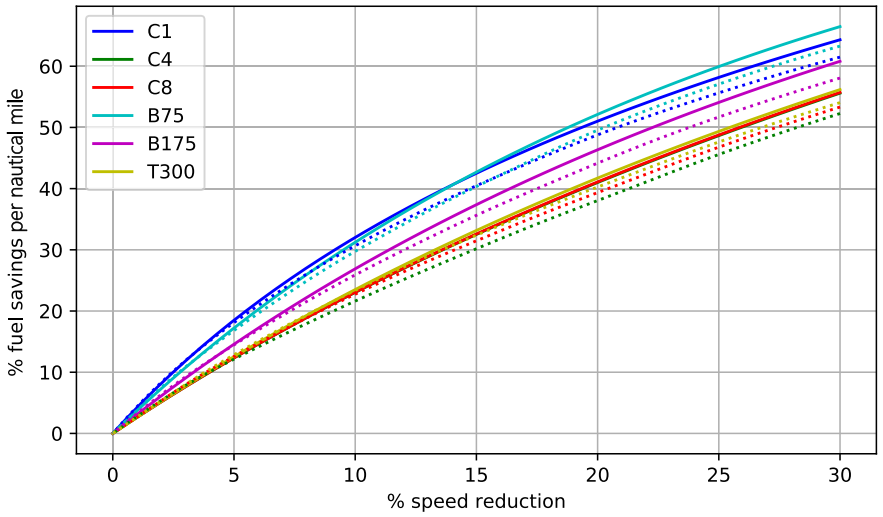

Fig. 13. The effect of considering variation of specific fuel consumption at different engine loads on relationship between speed reduction and fuel savings. (solid lines: considering constant SFOC; dotted lines: considering load dependent SFOC).

SFOC is lowest at 70% of MCR. Voyages have been simulated at different speeds, and fuel consumption is computed considering the SFOC variation at different loads.

The effect of load-dependent SFOC on fuel savings at different ship speeds can be seen in Fig. 13. When the variation of SFOC is considered, fuel savings drop by around 3% at 30% speed reduction. One can conclude that the effect of a drop in engine efficiency at low loads is relatively small.

7.3. Impact of varying weather conditions

The analysis so far has been performed in calm water which is rather an exception in reality. It is essential to estimate the influence of weather on fuel consumption at different ship speeds. As mentioned earlier, added resistance due to waves does not vary significantly with ship speed (Fig. 6). Especially at low speeds, added resistance due to waves can be a significant part of total resistance. Only a few studies like Lindstad et al. (2011) have considered the effect of averaged wind and waves in the transport model.

Voyages have been simulated on a route from Los Angeles to Osaka in average weather conditions of January, March, July, and October. The months have been selected to obtain maximum variation in weather conditions. Weather in terms of significant waveheight and peak periods at multiple points along the route can be seen in Fig. 3. The weather is rough in January and March whereas it is relatively calm in July.

The engine model and load-dependent SFOC have been considered in the voyage simulations. Fuel consumption for a complete

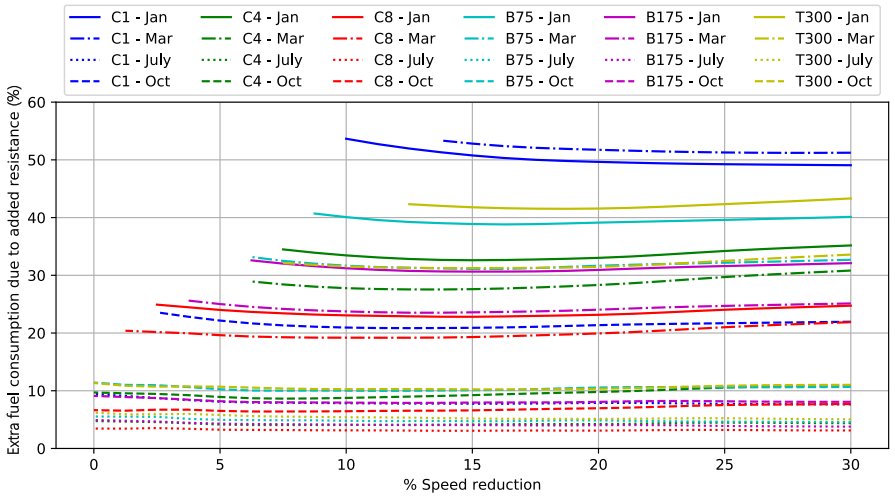

Fig. 14. Extra fuel consumption due to added resistance in waves as a percentage of fuel consumption in calm water at design speed. DTU method has been used for the calculation of added resistance.

voyage has been calculated at different ship speeds (FC_{wave}). Fuel consumption has also been computed assuming calm water conditions on the route (FC_{calm}) and fuel consumption due to added resistance in waves has been obtained as FC_{wave}-FC_{calm}. An increased bunker consumption due to waves as a percentage of fuel consumption at design speed in calm water can be seen in Fig. 14. The quantity plotted in Fig. 14 is obtained as follows:

$$\frac{FC(wave, V_1) - FC(calm, V_1)}{FC(calm, V_0)} \times 100$$

where, FC is fuel consumption in calm water or the presence of waves (*calm* or *wave*). V_0 is the design speed of the ship and V_1 is the speed at which the voyage is simulated.

The extra fuel consumption for a voyage because of rough weather is nearly independent of ship speed. The seasonal variation in the extra fuel requirement is much larger than the effect of varying ship speed. This means that reducing the ship speed only decreases the voyage fuel consumption related to calm water resistance. Notice that the fuel consumption calculated in this study are for a complete voyage.

A couple of different effects are at play here. As we have seen, added resistance decreases with ship speed (Fig. 6). However, reducing the speed leads to longer voyage time, therefore, higher fuel consumption. The effect of reduction in added resistance (or power) is compensated by an increased voyage time. Therefore, fuel consumption due to the presence of waves is independent of the ship speed. From this observation, one can conclude that added resistance in irregular waves decreases linearly with ship speed.

In certain weather conditions, engine power is insufficient to keep the speed constant over the whole voyage. The values have been plotted only for the cases where the entire voyage could be performed at a constant speed. Therefore, some of the plots in Fig. 14

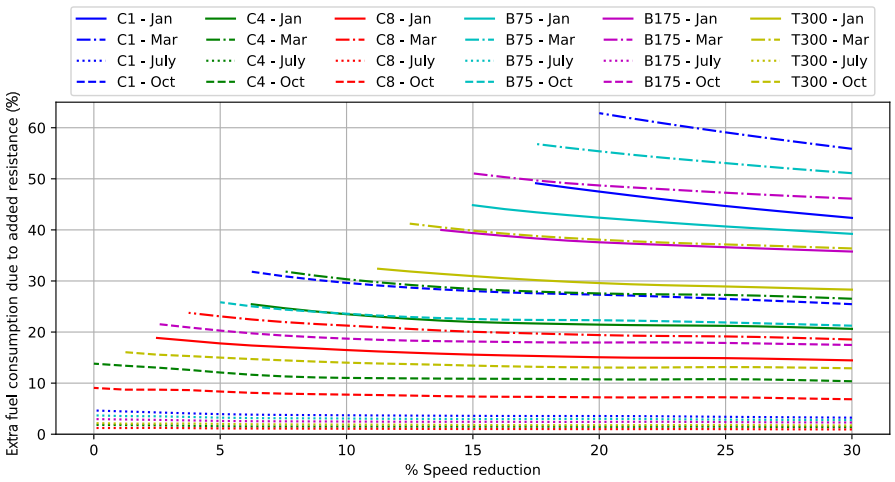

Fig. 15. Extra fuel consumption due to added resistance in waves as a percentage of fuel consumption in calm water at design speed. STAwave-2 method has been used for the calculation of added resistance.

do not start from 0% speed reduction. E.g. in the average weather of January, maximum possible speed is 10% lower than the design speed for C1 due to involuntary speed loss. Although in practice, it is common to keep power or RPM constant, constant speed simulations have been used for the ease of analysis.

One might wonder if these results are due to the specific method (DTU method) used for the calculation of added resistance. Therefore similar calculations have been performed using the empirical method STAwave-2 suggested by ITTC (2014). STAwave-2 considers head waves and waves coming from $\pm 45^{\circ}$ off the bow. Waves from other directions are neglected. Additional fuel consumption due to waves, calculated using STAwave-2 method has been plotted in Fig. 15. The order of magnitude of increased fuel consumption is similar to that in Fig. 14. In a few cases, e.g. C1 in March, the extra fuel consumption depends on ship speed. However, weather dependence is much larger than the speed dependence. Both the added resistance methods show that the additional bunker consumption for the voyage due to bad weather is independent of the ship speed. The impact of added resistance formulations on fuel consumption has been investigated by Taskar et al. (2019b).

The extra fuel consumption due to added resistance in waves can be significant as seen in Fig. 14. Therefore the effect of weather conditions should be included in shipping transport models. The observation that the voyage fuel consumption due to waves is independent of ship speed can be utilized in transport models as well as weather routing algorithms. A weather-dependent constant can be added to the fuel consumption instead of computing added resistance in waves at multiple points to obtain power and fuel consumption (as in Lindstad et al. (2011)). The accuracy of transport models can be greatly improved by considering weather conditions without increasing the complexity and required resources.

Plots of fuel savings vs speed reduction in different weather conditions can be seen in Fig. 16 and 17. The values have been plotted only for the cases where the entire voyage could be performed at a constant speed. Therefore, some of the plots do not start from 0% speed reduction. It can be observed that the benefits of speed reduction are highly weather-dependent. The estimated fuel savings can reduce by 30% in rough weather. As fuel consumption due to added wave resistance does not depend on ship speed, the benefits are greatest in calm weather. Reducing the ship speed sharply reduces the fuel consumption related to the calm water resistance as previously shown. Therefore, the estimation of fuel savings in calm water will always overestimate the benefits of speed reduction. Weather conditions are crucial to properly determine the effects of changing ship speed on fuel consumption and emissions. It is important to keep in mind that the analysis has been performed in monthly averaged weather conditions and not in extreme weather.

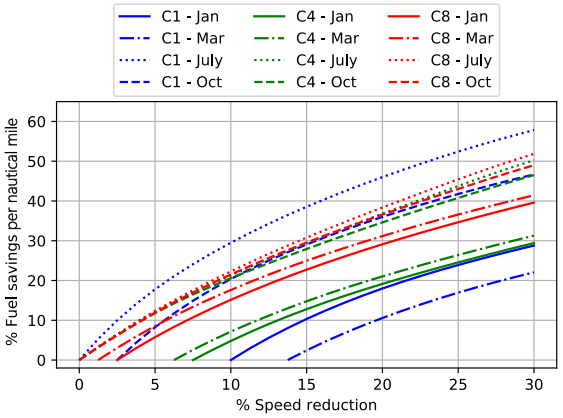

Fig. 16. Fuel savings due to speed reduction considering different weather conditions for the studied container vessels.

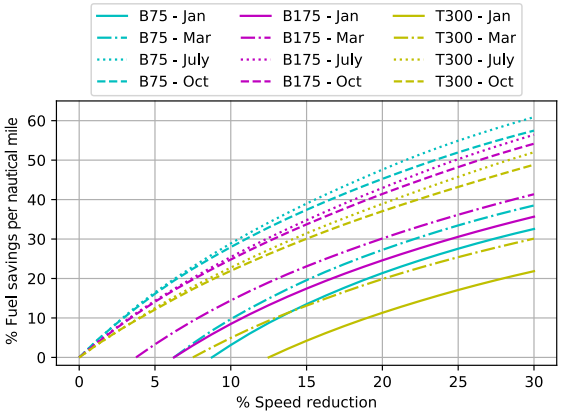

Fig. 17. Fuel savings due to speed reduction considering different weather conditions for the studied bulk carriers and tanker.

Weather dependence also varies for different ships. Container ship C1 shows the largest variation in fuel savings in different seasons (10–46% at 20% speed reduction), whereas, fuel savings of the container ship C8 do not vary significantly in different months (29–38% at 20% speed reduction). Weather dependent variation in fuel consumption for bulk carrier B75 and tanker T300 is around 30%, whereas B175 shows a slightly smaller variation (20%).

7.4. Effect of keeping yearly transport work constant

Speed reduction also reduces the transport work. In the view of growing trade, any limit on ship speed will lead to an increase in the number of ships needed to fulfill the transport demand. Fuel consumption and emission due to these additional ships should be considered while assessing the potential of speed reduction. Therefore, the analysis has been performed to study fuel savings due to speed reduction.

Fuel consumption has been corrected by considering additional ships required to keep yearly transport work constant. E.g. reducing speed to the half will need double the number of ships, therefore, fuel consumption at reduced speed must be doubled. The correction in fuel consumption is inversely proportional to the reduced ship speed as follows:

$$FC_{corrected} = FC \times \frac{V_0}{V_1}$$

where FC is an actual fuel consumption obtained from voyage simulation. V_1 is the reduced ship speed. V_0 is the design speed or the maximum speed that can be kept constant over a whole voyage, whichever is lower.

As seen in Fig. 18 and Fig. 19, fuel savings drop significantly as compared to the previous computations. The effect of weather conditions seems to be amplified. In the case of ship C1, a 30% speed reduction can lead to 4% to 40% fuel savings based on the weather conditions. (It is 22–57% without correcting the fuel consumption). A similar variation can be seen in the case of tanker T300.

These results are useful for assessing the prospects of emission reduction using speed reduction as a long term strategy. The yearly transport work has been kept constant even though transport demand has been predicted to rise by 3.8% annually (UNCTAD, 2018).

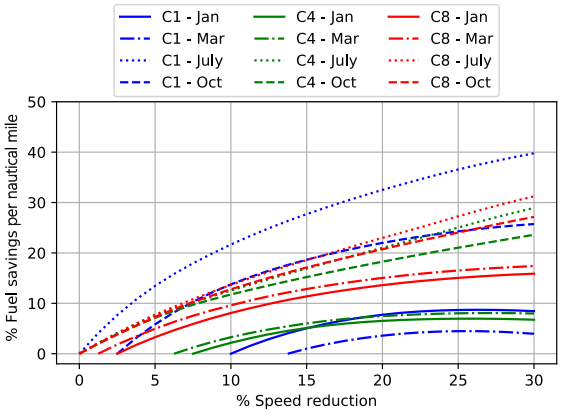

Fig. 18. Corrected fuel savings as a function of speed reduction in different seasons for the studied container vessels.

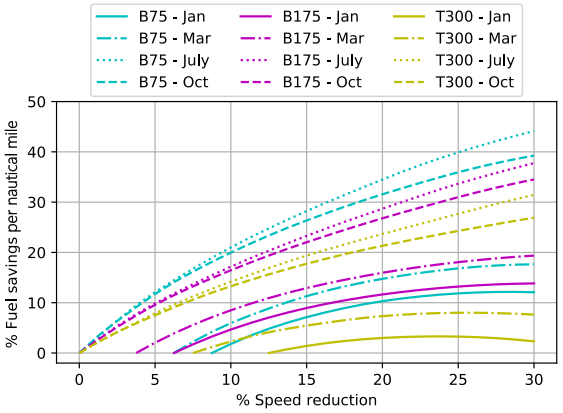

Fig. 19. Corrected fuel savings as a function of speed reduction in different seasons for the studied bulk carriers and tanker.

Table 4
Auxiliary engine load at sea.

Ship name	C1	C4	C8	B75	B175	T300
Auxiliary engine load (*kW*)	820	1390	1630	420	420	1500

The emissions caused during the construction of additional ships have been neglected as emissions in the shipbuilding phase are much smaller than those in the operation phase (Chatzinikolaou and Ventikos, 2013; Kameyama et al., 2007).

7.5. Effect of auxiliary engine fuel consumption

The analysis so far has considered power and fuel consumption required for propulsion alone. However, voyage fuel consumption will also get affected due to auxiliary engines on board the ships. It is much easier to consider the fuel consumption of auxiliary engines as it depends only on voyage time.

Simulations have been performed to check, how fuel savings per nautical mile get affected by considering auxiliary engine fuel consumption. Auxiliary engine loads for the ships at sea have been taken from Smith et al. (2015); the values have been presented in Table 4. It is assumed that all the auxiliary engines are 4-stroke medium speed engines, with SFOC of 200 g/kWh (Kristensen and Psaraftis, 2015). Auxiliary engine load is considered constant at different ship speeds.

As expected, fuel savings per nautical mile reduce when auxiliary engines are taken into consideration. Fuel savings corrected for additional ships including the effect of auxiliary engines have been presented in Fig. 20 and Fig. 21. The inclusion of auxiliary engines has an observable impact on fuel savings. In a few cases, especially for container ships, fuel savings start to decrease if the ship speed is reduced beyond a certain value.

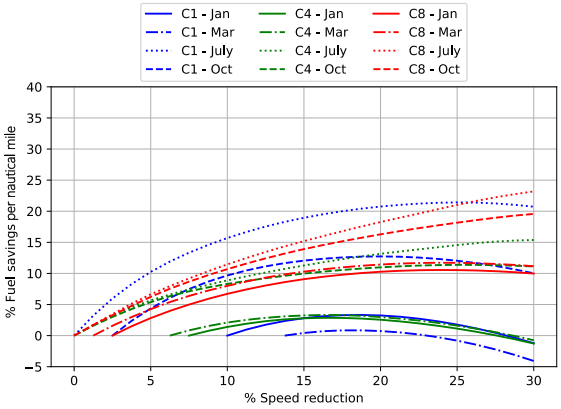

Fig. 20. Corrected fuel savings as a function of speed reduction in different seasons considering the auxiliary engine load for the studied container vessels.

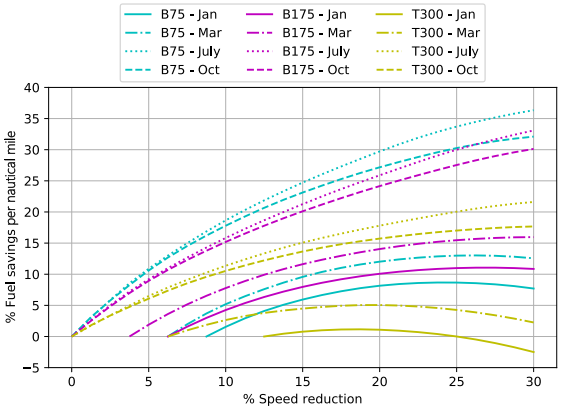

Fig. 21. Corrected fuel savings as a function of speed reduction in different seasons considering the auxiliary engine load for the studied bulk carriers and tanker.

8. Conclusions

- Assuming cubic relation between power and ship speed can cause a significant error (up to 15% for 30% speed reduction) in the calculation of fuel savings by speed reduction. The speed-power curve depends highly on ship size, type, and operating speed. A significant variation in the speed exponent was observed both among the ships and at different speeds. Therefore, the accurate speed-power curve should be used to calculate fuel consumption at different ship speeds.
- Variation in engine efficiency at different loads does not significantly affect fuel consumption at low ship speeds (up to 3%). Therefore, it is often acceptable to assume constant SFOC while studying the effect of ship speed on emissions and fuel consumption.
- Potential fuel savings by reducing the speed are highly dependent on weather conditions. However, it was observed that the additional fuel consumption for a voyage due to waves does not depend on ship speed. Speed reduction leads to a decrease in fuel consumption related to calm water resistance, whereas fuel consumption due to added resistance in waves remains unchanged. Therefore, fuel savings at reduced speed are larger in calm weather and much smaller in rough weather conditions.
- Keeping yearly transport work constant has a notable influence on the fuel-saving potential of speed reduction strategy.

CRediT authorship contribution statement

Bhushan Taskar: Conceptualization, Formal analysis, Investigation, Methodology, Software, Validation, Visualization, Writing - original draft, Writing - review & editing. **Poul Andersen:** Conceptualization, Funding acquisition, Project administration, Supervision.

Acknowledgments

The authors thank Orients Fund, The Danish Maritime Fund and Department of Mechanical Engineering, Technical University of Denmark, for their financial support of this work.

Appendix A. Supplementary material

Supplementary data associated with this article can be found, in the online version, at https://doi.org/10.1016/j.trd.2020.102337. It can also be accessed at https://doi.org/10.11583/DTU.12012024.

References

Bertram, V., Chao, K.-Y., Lammers, G., Laudan, J., 1994. Experimental validation data of free-surface flows for cargo vessels. In: Proceedings of the CFD workshop, vol. 1, Tokyo, pp. 311–320.
BSRA, 1971. Methodical series experiments on single-screw ocean-going merchant ship forms. Extended and revised overall analysis. Technical Report. BSRA Report NS, 333.
Chatzinikolaou, S.D., Ventikos, N.P., 2013. Assessment of ship emissions in a life cycle perspective. In: 3rd International Energy, Life Cycle Assessment, and Sustainability Workshop & Symposium (ELCAS3), Nisyros, Greece.
Copernicus Climate Change Service (C3S), 2017. ERA5: Fifth generation of ECMWF atmospheric reanalyses of the global climate. Copernicus Climate Change Service Climate Data Store (CDS). https://www.ecmwf.int/.
Corbett, J.J., Wang, H., Winebrake, J.J., 2009. The effectiveness and costs of speed reductions on emissions from international shipping. Transp. Res. Part D: Transp. Environ. 14, 593–598. https://doi.org/10.1016/j.trd.2009.08.005.
Du, Y., Chen, Q., Quan, X., Long, L., Fung, R.Y., 2011. Berth allocation considering fuel consumption and vessel emissions. Transp. Res. Part E: Logist. Transp. Rev. 47, 1021–1037. https://doi.org/10.1016/j.tre.2011.05.011.
el Moctar, O., Shigunov, V., Zorn, T., 2012. Duisburg test case: Post-panamax container ship for benchmarking. Ship Technol. Res. 59, 50–64. https://doi.org/10.1179/str.2012.59.3.004.
Faber, J., Nelissen, D., Hon, G., Wang, H., Tsimplis, M., 2012. Regulated slow steaming in maritime transport: An assessment of options, costs and benefits, CE Delft, Delft, February 2012.
Fagerholt, K., Laporte, G., Norstad, I., 2010. Reducing fuel emissions by optimizing speed on shipping routes. J. Oper. Res. Soc. 61, 523–529. https://doi.org/10.1057/jors.2009.77.
Faltinsen, O.M., Minsaas, K.J., Liapis, N., Skjørdal, S.O., 1980. Prediction of resistance and propulsion of a ship in a seaway. In: 13th Symposium on Naval Hydrodynamics, Tokyo, pp. 505–529.
Guldhammer, H.E., Harvald, S.A., 1974. Ship Resistance - Effect of Form and Principal Dimensions. Akademisk Forlag, Copenhagen.
Harvald, S.A., 1983. Resistance and Propulsion of Ships. Wiley & Sons, New York.
ITTC, 1978. Recommended Procedures and Guidelines 7.5-02-03-01.4, 1978 ITTC Performance Prediction Method, 2014. Effective Date 2014, Revision 03.
ITTC, 2014. Recommended Procedures and Guidelines 7.5-04-01-01.2. Analysis of Speed/Power Trial Data, 2014. Effective Date 2014, Revision 01.
Kameyama, M., Hiraoka, K., Tauchi, H., 2007. Study on Life Cycle Impact Assessment for Ships. Technical Report 3. National Maritime Research Institute.
Kristensen, H.O.H., 2012. Model for environmental assessment of container ship transport. Trans. Soc. Naval Archit. Marine Eng. 118, 122–139.
Kristensen, H.O., 2018. Speed and emission reduction from ships. Naval Architect 2018, 40–44.
Kristensen, H.O., Bingham, H., 2015. Revision of statistical analysis and determination of regression formulas for main dimensions of container ships based on data from Clarkson Technical Report. URL https://gitlab.gbar.dtu.dk/oceanwave3d/Ship-Desmo.
Kristensen, H.O., Bingham, H., 2015. Revision of statistical analysis and determination of regression formulas for main dimensions of bulk carriers based on data from Clarkson. Technical Report. URL https://gitlab.gbar.dtu.dk/oceanwave3d/Ship-Desmo.
Kristensen, H.O., Bingham, H., 2015. Revision of statistical analysis and determination of regression formulas for main dimensions of tankers based on data from Clarkson. Technical Report. URL https://gitlab.gbar.dtu.dk/oceanwave3d/Ship-Desmo.
Kristensen, H.O., Bingham, H., 2017. Prediction of Resistance and Propulsion Power of Ships. Technical Report. Technical University of Denmark. URL https://gitlab.gbar.dtu.dk/oceanwave3d/Ship-Desmo.
Kristensen, H.O., Psaraftis, H.N., 2015. Energy demand and exhaust gas emissions of marine engines. Technical Report. URL https://gitlab.gbar.dtu.dk/oceanwave3d/

Ship-Desmo.
Lee, C.-H., Newman, J.N., 2013. WAMIT user manual, version 7.0. http://www.wamit.com/manual.htm.
Lindstad, H., Eskeland, G.S., 2015. Low carbon maritime transport: How speed, size and slenderness amounts to substantial capital energy substitution. Transp. Res. Part D: Transp. Environ. 41, 244–256. https://doi.org/10.1016/j.trd.2015.10.006.
Lindstad, H., Asbjørnslett, B.E., Strømman, A.H., 2011. Reductions in greenhouse gas emissions and cost by shipping at lower speeds. Energy Policy 39, 3456–3464. https://doi.org/10.1016/j.enpol.2011.03.044.
Larsson, L., Stern, F., Visonneau, M. (Eds.), 2014. Numerical Ship Hydrodynamics - An assessment of the Gothenburg 2010 Workshop. Springer. https://doi.org/10.1007/978-94-007-7189-5.
Lindstad, H., Asbjørnslett, B.E., Jullumstrø, E., 2013. Assessment of profit, cost and emissions by varying speed as a function of sea conditions and freight market. Transp. Res. Part D: Transp. Environ. 19, 5–12. https://doi.org/10.1016/j.trd.2012.11.001.
MAN Diesel & Turbo, 2013. Propulsion trends in container vessels. Technical Report.
MAN Diesel & Turbo, 2013. Propulsion trends in tankers. Technical Report.
MAN Diesel & Turbo, 2014. Propulsion trends in bulk carriers. Technical Report.
MAN Energy Solutions, 2018. Basic principles of ship propulsion. Technical Report.
MAN Energy Solutions, 2019. CEAS Engine Calculations. https://marine.man-es.com/two-stroke/ceas (accessed on 30 Oct. 2019).
Martinsen, M.A., 2016. An design tool for estimating the added wave resistance of container ships. Master's thesis. Technical University of Denmark. URL https://findit.dtu.dk/en/catalog/2306945831.
Molland, A.F., Turnock, S.R., Hudson, D.A., 2011. Ship Resistance and Propulsion. https://doi.org/10.1017/CBO9780511974113.
Nielsen, C.S., 2015. A Ship Design Support Tool for Estimating Added Resistance in Waves. Master's thesis. Technical University of Denmark. URL https://findit.dtu.dk/en/catalog/2292735707.
Norlund, E.K., Gribkovskaia, I., 2013. Reducing emissions through speed optimization in supply vessel operations. Transp. Res. Part D: Transp. Environ. 23, 105–113. https://doi.org/10.1016/j.trd.2013.04.007.
Olmer, N., Comer, B., Roy, B., Mao, X., Rutherford, D., 2017. Greenhouse gas emissions from global shipping, 2013–2015. Int. Counc. Clean Transp. 1–38.
Psaraftis, H.N., Kontovas, C.A., 2009. CO_2 emission statistics for the world commercial fleet. WMU J. Marit. Affairs 8, 1–25. https://doi.org/10.1007/BF03195150.
Psaraftis, H.N., Kontovas, C.A., 2013. Speed models for energy-efficient maritime transportation: A taxonomy and survey. Transp. Res. Part C 26, 331–351. https://doi.org/10.1016/j.trc.2012.09.012.
Salvesen, N., 1978. Added resistance of ships in waves. J. Hydronaut. 12, 24–34.
Schneekluth, H., Bertram, V., 1998. Lines design. In: Ship Design for Efficiency and Economy, second ed. Butterworth-Heinemann, pp. 34–84. doi:https://doi.org/10.1016/B978-075064133-3/50002-5 (Chapter 2).
Smith, T.W.P., Jalkanen, J.P., Anderson, B.A., Corbett, J.J., Faber, J., Hanayama, S., O'Keeffe, E., Parker, S., Johansson, L., Aldous, L., Raucci, C., Traut, M., Ettinger, S., Nelissen, D., Lee, D.S., Ng, S., Agrawal, A., Winebrake, J.J., Hoen, A., Chesworth, M.S., Pandey, A., 2015. Third IMO Greenhouse Gas Study 2014.
UNCTAD, 2018. Review of maritime transport 2018. UNCTAD/RMT/2018.
Taskar, B., Regener, P.B., Andersen, P., 2019a. The impact of propulsion factors on vessel performance in waves. In: Felli, Mario, Leotardi, Cecilia (Eds.), Sixth International Symposium on Marine Propulsors - SMP'19. vol. 1 National Research Council of Italy, Institute of Marine Engineering (CNR-INM, Rome, Italy. https://findit.dtu.dk/en/catalog/2449928453.
Taskar, B., Regener, P.B., Andersen, P., 2019b. The impact of variation in added resistance computations on voyage performance prediction. In: Proceedings of the 14th International Symposium on Practical Design of Ships and Other Floating Structures (PRADS'19). Springer, Yokohama, Japan.
Wang, S., Meng, Q., 2012. Sailing speed optimization for container ships in a liner shipping network. Transp. Res. Part E: Logist. Transp. Rev. 48, 701–714. https://doi.org/10.1016/j.tre.2011.12.003.
Woo, J.K., Moon, D.S.H., 2014. The effects of slow steaming on the environmental performance in liner shipping. Marit. Policy Manage. 41, 176–191. https://doi.org/10.1080/03088839.2013.819131.